Mode emission properties of semiconductor micro-disk and micro-ring lasers

T.-D. Lee[a], P.-H. Cheng[a], J.-S. Pan[a], K. Tai[a], Y. Lai*[a], and K.-F. Huang[b]
[a]Institute of Electro-Optical Engineering, National Chiao-Tung University, Hsinchu, Taiwan, ROC
[b] Department of Electro-Physics, National Chiao-Tung University, Hsinchu, Taiwan, ROC

ABSTRACT

We have successfully fabricated optically pumped semiconductor micro-disk and micro-ring lasers under the InGaAsP/InGaAs system at the 1.5μm wavelength and under the InGaP/InGaAlP system at the 0.66 μm wavelength. The spontaneous emission factor β of these micro-lasers is estimated directly from their output-pump curves and its dependence on the cavity volume is verified. Interesting phenomena regarding the far-field emission pattern and lasing linewidth of these micro-cavity lasers are experimentally observed and theoretically studied.

Keywords: Micro-cavity laser, Micro-disk laser, Micro-ring laser

1. INTRODUCTION

Semiconductor micro-disk and micro-ring lasers have attracted a lot of research interest recently due to their special properties including the high spontaneous emission factor β and the low lasing threshold [1-6]. In such micro-structures with their size comparable to the optical wavelength, the emission property of excited dipoles can be greatly altered compared to the emission properties in the bulk. The underlying physical cause is the quantitative change of the photonic density of states due to strong optical confinement, which is analogous to the electronic counterpart in the presence of strong quantum confinement. Such modification of the emission properties due to optical confinement automatically leads to a cavity-volume dependent spontaneous emission factor β for any micro-cavity laser. In the mean while, the lasing modes of a semiconductor micro-disk laser are whispering-gallery-modes (WGMs) that propagate along the edge of the disk. Due to such a special resonant structure, the emission properties of micro-disk lasers exhibit many interesting differences compared to typical edge emitting lasers. The aim of this paper is to report our recent results on investigating these interesting properties.

We have successfully fabricated optically pumped semiconductor micro-disk and micro-ring lasers under the InGaAsP/InGaAs system at the 1.5μm wavelength[7-9] and under the InGaP/InGaAlP system at the 0.66 μm wavelength[10]. The micro-disks can be fabricated either by the pedestal-suspended method illustrated in figure 1(a) or by the epi-transferred method illustrated in figure 1(b). On the other hand, the micro-rings can only be fabricated by the epi-transferred method since the suspended pedestal can not be formed for a micro-ring. Figure 1(c) and (d) shows the SEM pictures of a typical pedestal- suspended micro-disk laser and a typical epi-transferred micro-ring laser fabricated in our lab. One advantage of the epi-transferred method is that one can simultaneously fabricate micro-disks and micro-rings of different sizes using a same wafer such that the comparison of their properties can be more meaningful and trustable.

The first subject of our study is to investigate the cavity volume dependence of the spontaneous emission factor β [8,11,12]. We have developed a method that can extract the value of β directly from the measured output-pump curve. By experimentally fabricating a series of micro-ring lasers with different ring-widths on the same wafer and using the epi-transfer method, we verify experimentally the inverse cavity volume dependence of the spontaneous emission factor and achieve a β value as large as 0.14. To clarify the obtained results, we derived a simple expression based on the classical mode counting method, which can give a rough estimate of the β value without requiring detailed cavity mode calculation. The predictions from this expression agree quantitatively with the experimental results for both the InGaAsP/InGaAs micro-lasers at the 1.5μm wavelength and the InGaP/InGaAlP micro-lasers at the 0.66 μm wavelength.

The second subject of our study is to investigate the far-field emission patterns of semiconductor micro-disk lasers[9,13]. Experimentally we fabricate pedestal-suspended micro-disk lasers along the wafer cleaved edge so that the reflected lights

* Correspondence: E-mail: yclai@cc.nctu.edu.tw; Fax:886-3-5716631; Tel:886-3-5913077

Part of the SPIE Conference on Photonics Technology into the 21st Century:
Semiconductors, Microstructures, and Nanostructures • Singapore • December 1999
SPIE Vol. 3899 • 0277-786X/99/$10.00

from the substrate will not deteriorate the measurement. The far-field distributions along both the θ and ϕ directions are then measured by a scanning detector. Interesting results including far-filed emission angle narrowing along the θ direction and quasi-periodic distribution along the ϕ direction are observed. To explain the observed results, we have derived an expression for the far-filed distribution in the cylindrical coordinate based on the scalar diffraction theory. The predictions from this expression agree very well with the measured data. Rigorous calculation based on the vector diffraction theory also yields similar results.

The third subject of our study is to investigate the lasing linewidths of a semiconductor micro-cavity laser under different pumping levels[14]. Interesting pump-power dependence of the lasing linewidths is observed for both the micro-disk and micro-ring lasers. We find that the usual theory of laser linewidth is not enough for explaining the results we observe.

The fourth subject of our study is to investigate the emission properties of non-circular micro-lasers[15]. We have successfully fabricated semiconductor micro-cavity lasers that have non-circular shapes (i.e., a pentagon shape micro-cavity laser). Optical lasing still can be achieved for these non-circular micro-cavity lasers. Again their far-filed distributions are measured and are found to exhibit interesting properties.

In the following we shall present the details of our experimental and theoretical results on the above four subjects. We will also point out some unexplained phenomena that we observed.

2. THE SPONTANEOUS EMISION FACTOR

The spontaneous emission factor β is defined as the fraction of the spontaneous emission that falls into the cavity mode[11,12],

$$\beta \equiv \frac{\gamma_c}{\gamma_{sp}} \tag{1}$$

where γ_c is spontaneous emission rate into the cavity mode and γ_{sp} is the net spontaneous emission rate. For a monochromatic dipole, the Fermi golden rule gives the following expression for γ_c:

$$\gamma_c = \frac{2\pi}{\hbar^2}\mu^2 E^2(\vec{r}_a)\rho_c(\omega) \tag{2}$$

Here μ is the dipole moment, and $E(\vec{r}_a)$ is the vacuum field amplitude at the position of the dipole. Since

$$\int dV \varepsilon E^2(\vec{r}) = \frac{\hbar\omega}{2} \tag{3}$$

As an estimate, one can assume

$$E^2(\vec{r}_a) = \frac{\hbar\omega}{2\varepsilon_o n^2 V_m} \tag{4}$$

with V_m being the cavity mode volume. In Eq.(2), ρ_c is the optical density of the state and can be simply estimated by: $\rho(\omega) = 1/\Delta\omega_c$, with $\Delta\omega_c$ being the linewidth of the cold optical cavity. Practically the dipole will have a finite spontaneous emission linewidth $\Delta\omega_{sp}$. If $\Delta\omega_{sp} << \Delta\omega_c$, the dipole is effectively monochromatic and Eq.(2) is applicable. However, if $\Delta\omega_{sp} > \Delta\omega_c$, we need to multiply the spectral overlap factor $\Delta\omega_c / \Delta\omega_{sp}$ into Eq.(2) to take into account the spectral broadening effect. For our micro-disks and micro-rings, $\Delta\lambda_{sp}$ is about 30 nm and $\Delta\lambda_c$ is about 1 nm, therefore this spectral overlay factor is needed. Please also note that the mode volume V_c is not necessarily the cavity volume V_m. Actually $V_m \approx V_c w_R / R$ for a disk, where w_R is the width of the whispering gallery mode and R is the disk radius. To account for the spatial overlap effect between the mode field and the dipole distribution, we need to add a spatial overlap factor V_m / V_c in Eq.(2). Finally, it is reasonable to assume that the total spontaneous emission rate γ_{sp} for practical semiconductor micro-disks and micro-rings is roughly the same as the bulk value:

$$\gamma_{sp} = \gamma_b = \frac{\mu^2 \omega^3 n}{3c^3 \hbar \varepsilon_o \pi} \tag{5}$$

With these expressions, we finally obtain

$$\beta = \frac{\lambda}{8\pi \Delta\lambda_{sp}} \left(\frac{\lambda}{n}\right)^3 \frac{1}{V_c} \tag{6}$$

In getting Eq.(6), we have multiplied the result by a factor of 1/3 to account for the randomness in dipole orientation. Eq.(6) actually contains an interesting physical interpretation: the mode counting concept. If we define N_m as the number of mode that a cavity can support, then a reasonable estimate of N will be the bulk density of state times the cavity volume times the dipole emission linewidth. After some algebra, it is easy to find that the β factor in Eq.(6) is simply equal to the reciprocal of N:

$$\beta = \frac{1}{N_m} \tag{7}$$

With this interpretation, one can estimate the β value simply by counting the mode. As an example, let us consider a micro-disk with a diameter of 3 μm. By following the conformal transform and WKB analyses detailed in the literature, we find that there exist four modes in the span of the dipole emission spectrum. The four modes have similar field distribution and are of very high Q. Therefore the mode-counting method will predict the β value to be 1/8 = 0.125. The additional factor of two is from the degeneracy of counterclockwise and clockwise traveling wave modes. When applying Eq.(7) directly, we obtain β = 0.121, where λ = 1.5 μm, $\Delta\lambda_{sp}$ = 30 nm, and n = 3.4 are used. The two values agree well with each other and also with the experimental result to be shown below. For a micro-ring, it supports fewer modes than a micro-disk of the same size and thus will has a larger β.

We now turn to the question about how to determine the β factor experimentally. From the rate equation model of a single-mode laser, the measured pumping power P_m and the measured lasing power P_L at the steady state satisfy the following expression[8]:

$$P_m = (c_1 / \beta) P_L (1 + \beta c_2 P_L) / (1 + c_2 P_L) \tag{8}$$

Here c_1 and c_2, are two unknown constants. By fitting the measured P_L versus P_m curve with this expression, one can determine the β value unambiguously. Figure 2(a) and (b) plot the obtained β values for micro-disk and micro-rings with different disk radius or ring widths. The inverse dependence of the β value on the disk radius or ring width is very obvious. The solid lines in both figures are the predictions from Eq.(6) . The agreement is very excellent.

3. THE FAR-FIELD PATTERN IN THE Θ DIRECTION

Figure 3(a) illustrates our experimental setup for measuring the far-field distribution. The measured distributions along the θ direction for micro-disks with two different radius are shown in figures 3(b) and (c). The symmetric distribution of the two figures indicates that the reflected lights from the substrate do not interfere our measurement. One special point about the two figures is that the far-field emission angle along the θ direction is much narrower than the prediction from the Fraunhofer diffraction formulation. The thickness of our micro-disk lasers at the 1.5 μm wavelength is 0.2 μm, which is much narrower than the optical wavelength. One would thus expect that the emission angle spreading along the θ direction will be very large according to the Fraunhofer diffraction formulation, but this is not what we observed in figures 3(b) and (c). In order to explain the observed results, we have developed a new far-field diffraction formulation in the cylindrical coordinate based on the scalar diffraction theory and the stationary phase approximation. The final far-field intensity distribution along the θ direction is given by[9]:

$$I(\theta) \propto \left| \frac{F(k\cos\theta)}{H_m^{(2)}(kR\sin\theta)} \right|^2 \tag{9}$$

where R is the disk radius and $F(k_z)$ is the inverse Fourier transform of the near-field distribution. Eq.(9) is to be compared with the result from the Fraunhofer diffraction formulation. The Fraunhofer diffraction theory is derived for a planar near-field distribution and the far-field intensity distribution is given by:

$$I(\theta) \propto \left|F(\sqrt{k^2 - k_y^2}\cos\theta)\right|^2 = \left|F(k_z)\right|^2 \tag{10}$$

The main difference between the two expressions is that an additional factor proportional to the inverse square of the Hankel function appears in Eq.(9). This additional factor signifies the geometry difference between a planar near-field distribution and a cylindrical near-field distribution. For practical micro-disks, this additional geometry factor in fact dominates in determining the emission angle θ_{FWHM}. Figure 3(d) shows the comparison between the theoretical predictions from Eq.(9) and the experimental results from figure 3(b) and (c). The agreement is very excellent. We have also performed another calculation based on the more rigorous vector diffraction theory. The obtained results are also similar, as also have been shown in figure 3(d). Our vectorial analysis also verifies that the polarization of the far-filed is mainly along the ϕ direction, which again agree with experimental observations.[16]

4. THE LASING WAVELENGTHS AND LINEWIDTHS UNDER DIFFERENT PUMP LEVELS

In this section we present our experimental data on the pump power dependence of the single mode lasing wavelengths and linewidths for both micro-disk and micro-ring lasers. Figure 4 shows a series of experimentally measured single mode emission wavelengths versus the pumping power for 3, 5, 8 μm diameter micro-disks and a 5 μm diameter micro-ring. The horizontal axis is the pump power in unit of the threshold pump power, P_{th}. We notice that the emission wavelength is blue shifted as the pump increases. This is in accordance with the usual carrier dependent index effect. As the pump increases further, the wavelength becomes red shifted. Presumably this is due to the thermal effect. Figure 5 shows the corresponding emission linewidth versus pumping power for the same devices used to obtain figure 4. The data points are plotted in solid squares. Again, the horizontal axis is the pump power in unit of the threshold pump power, P_{th}. It is expected that the linewidth will decrease as the pump power increases from zero to the threshold value. The reduction by a factor of 10 is observed for the 8 μm diameter micro-disk at the vicinity of threshold. However, the linewidth remains almost unchanged as the pump increases further. This is different from the cases of conventional single mode semiconductor DFB and DBR lasers, which show the inverse proportionality with the output power when the alsers are pumped above the threshold. However, our observation agrees with the report of Mohideen et al[14]. They attributed this finding to strong interplay with the carrier dynamics when the spontaneous and stimulated emission rates at large β are comparable to the carrier equilibration rates. Theoretical calculation of the laser linewidth based on the single mode rate equation analysis gives a well-known expression for the laser linewidth:

$$\Delta\nu = \frac{1}{2\pi}[\gamma_c - \beta r_{sp}(N - N_0)] \qquad \text{below threshold} \tag{11}$$

$$\Delta\nu = \frac{1}{2\pi}[\gamma_c - \beta r_{sp}(N - N_0)]\frac{(1+\alpha^2)}{2} \quad \text{above threshold} \tag{12}$$

where α is the lenewidth enhancement factor, N is the carrier number and N_0 is the transparent carrier number. Results from Eq.(11) and (12) are plotted in solid lines and are superimposed with the experimental data in figure 5. It is clear that the agreement is good only when the pump power is near or less than the threshold pumping value. Our study indicates that the analysis based on Henry and Schawlow-Townes linewidth formulation is not adequate for the semiconductor micro-disks or micro-rings. More sophisticate analyses are needed in order to explain these observed results.

5. NON-CIRCULAR MICRO-LASERS AND THE FAR-FIELD PATTERN IN THE ϕ DIRECTION

To investigate the possibility of obtaining highly directional output lights[15], we have fabricated micro-cavity lasers of a pentagon shape under the InGaAsP/InGaAs system at the 1.55 μm wavelength. The fabrication procedures are the same as described in Section 1 except a pentagon mask pattern is used. Figure 6(a) shows the SEM of a 8 μm outer-diameter pentagon micro-laser right on the edge of the cleaved wafer. Optical lasing still can be achieved for this type of lasers. The lasing spectra as well as the output versus pump curve are shown in figure 6(b) and (c). The experimental results we observed do not give an obvious 5-peaks far-field distribution around the ϕ direction, as one might expect intuitively. Instead, the measured far-field emission distribution exhibits quasi-periodic distribution as shown in figure 6(d). Similar quasi-periodic distributions actually also exhibit in the measured results for circular micro-disks of different disk radius, as have been shown in figure 6(e) and (f). The period of the quasi-periodic distributions is a function of the disk radius and is not equal to the period of the standing wave pattern as one might expect. We are still searching for a reasonable explanation for these observed results.

6. CONCLUSIONS

We have presented the results of our recent investigation on semiconductor micro-disk and micro-ring lasers. Properties about the spontaneous emission factor and the far-filed emission pattern of these micro-lasers have been clarified both experimentally and theoretically. Some interesting results about the lasing linewidth and the far-filed distribution along the ϕ direction are experimentally observed and further studies are needed. We hope these results can serve as a basis for future investigation along this direction.

ACKNOWLEDGMENTS

This research was supported in parts by National Science Council of Taiwan, R.O.C.

REFERENCES

1. S. L. McCall, A. F. Levi, R. E. Slusher, S. J. Pearton, and R. A. Logan, "Whispering-gallery mode microdisk lasers," Appl. Phys. Lett. **60**, pp.289-291, 1992.
2. A. F. levi, R. E. Slusher, S. L. McCall, T. Tanbun-Ek, D. L. Coblentz and S. J. Pearton, "Room temperature operation of microdisk lasers with submilliamp threshold current," Electron. Lett., **28**, pp.1010-1011, 1992.
3. M. J. Rise, E. I. Chen, N. Holonyak, Jr., G. M. Iovino and A. D. Minervini, "Planar native-oxide-based AlGaAs-GaAs-InGaAs quantum microdisk lasers," Appl. Phys. Lett. **68**, pp.1540-1542, 1996.
4. M. Fujita, K. Inoshita and T. Baba, "Room temperature continuous wave lasing characteristics of GaInAsP/InP microdisk injection laser", Electron. Lett. **34**, pp.278-279, 1998.
5. B. Corbett, J. Justice, L. Considine, S. Walsh, and W. M. Kelly, "Low-threshold lasing in novel microdisk geometries,", IEEE Photonic Tech. Lett., **8**, p.855-857, 1996.
6. J. P. Zhang, D. Y. Chu, S. L. Wu, S. T. Ho. W. G. Bi, C. W. Tu, and R. C. Tiberio, "Photonic-wire laser," Phys. Rev. Lett., **75**, pp.2678--2681, 1995.
7. T. D. Lee, P. H. Cheng, J. S. Pan, K. Tai and Y. Lai. "Mode emission characteristics of semiconductor micro-disk and micro-ring lasers," Opt. Quant, Electron. **28**, pp.1335-1341, 1996.
8. P. H. Cheng, T.D. Lee, J. S. Pan, Y. Lai and K. Tai . "Spontaneous emission factor versus cavity volume in low dimensional photonic micro-cavities," Opt. Comm. **142**, p.229-233, 1997.
9. T. D. Lee, P. H. Cheng, J. S. Pan, R. S. Tsai, Y. Lai, and K. Tai. "Far-field emission narrowing effect of micro-disk lasers," Appl. Phys. Lett. **72**, pp.2223-2225, 1998.
10. J. S. Pan, P. H. Cheng, T. D. Lee, Y. Lai, and K. Tai. "0.66 μ mInGaP/InGaAlP single quantum-well micro-disk lasers," Japanese Journal of Applied Physics **37**, pp.643-645, 1998.
11. M. K. Chin,D. Y. Chu, and S. T. Ho, "Approximate solution of the whispering gallery modes and estimation of the spontaneous emission coupling factor for microdisk lasers," Opt. Comm. **109**, pp.467-471, 1994.
12. M. K. Chin, D. Y. Chu, and S. T. Ho, "Estimation of the spontaneous emission factor for microdisk lasers via the approximation of whispering gallery modes," J. Appl. Phys., **75**, pp.3302-3307, 1994.
13. B.-J. Li and P.-L Liu, "Analysis of Far-Field Patterns of microdisk resonators by the finite-difference time-domain Method," IEEE J. Quantum Electron., **33**, p.1489, 1997.
14. U. Mohideen, R. E. Slusher, F. Jahnke, and S. W. Koch, "Semiconductor microlaser linewidth," Phys. Rev. Lett. **73**, pp.1785-1788, 1994.
15. A. F. Levi, R. E. Slusher, S. L. McCall, J. L. Glass, S. J. Pearton, and R. A. Logan, "Directional light coupling from microdisk lasers," Appl. Phys. Lett. **62**, pp.561-563, 1993.
16. N. C. Frateschi, A. P. Kanjanmata, and A. F. Levi, "Polarization of lasing emission in microdisk laser diodes," Appl. Phys. Lett., **66**, p.1859-1861, 1995.

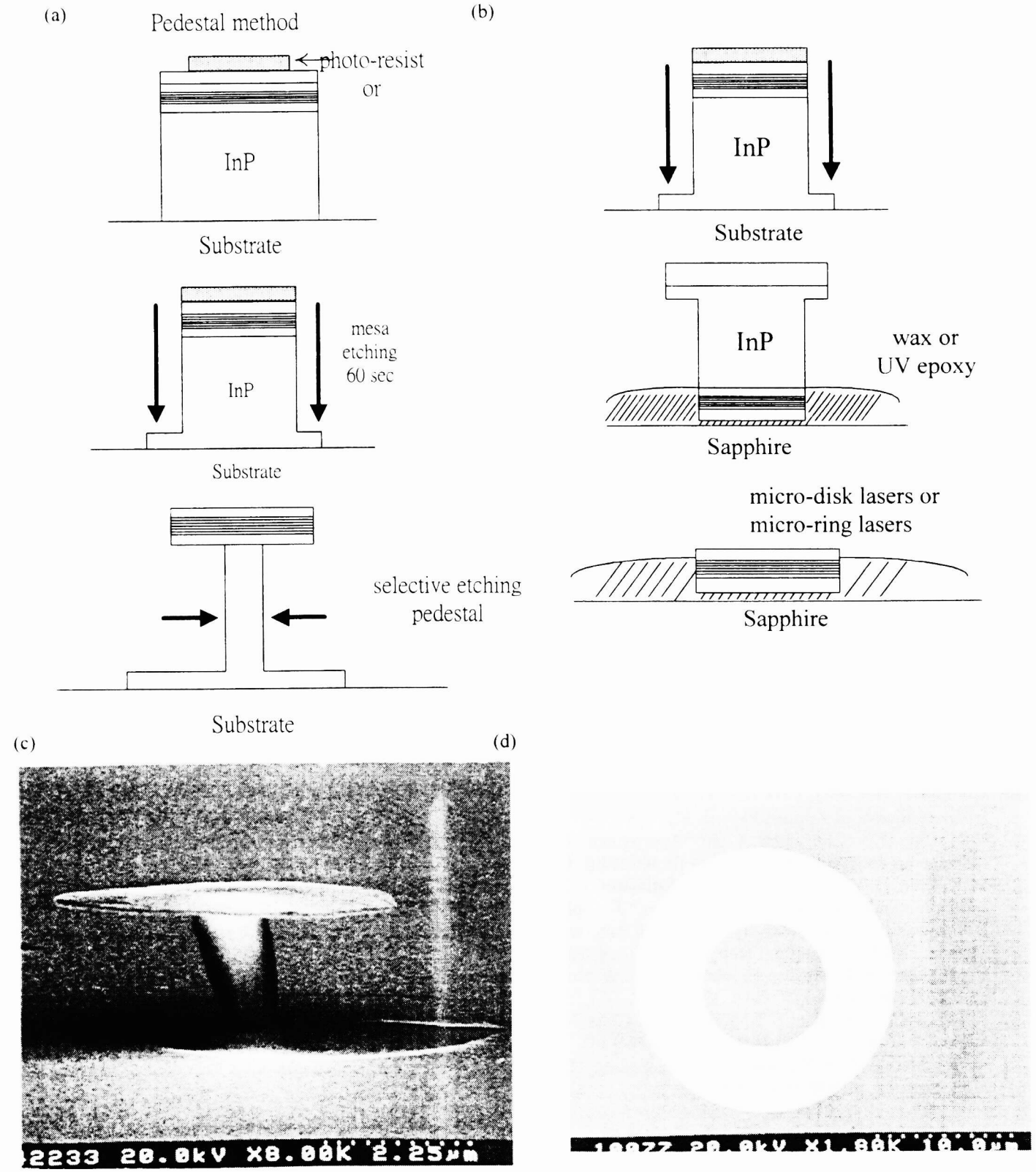

Figure 1: (a) Fabrication of pedestal suspended micro-disk lasers; (b) Fabrication of epi-transferred micro-disk or micro-ring lasers; (c) SEM of a pedestal suspended micro-disk; (d) SEM of a epi-transferred micro-ring.

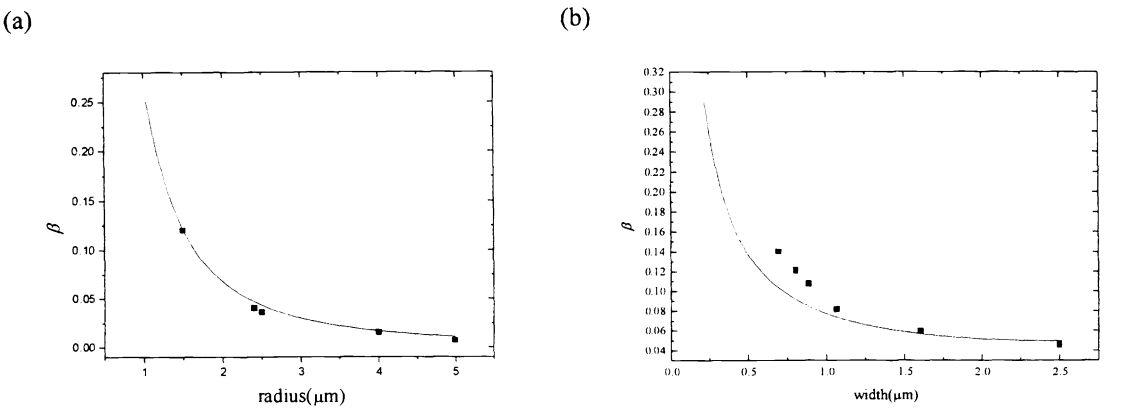

Figure 2: (a) The β values of micro-disk lasers with different radius; (b) The β values of micro-ring lasers with a same outer radius but different ring widths. Dot points: experimental data; Solid line: theoretical predictions.

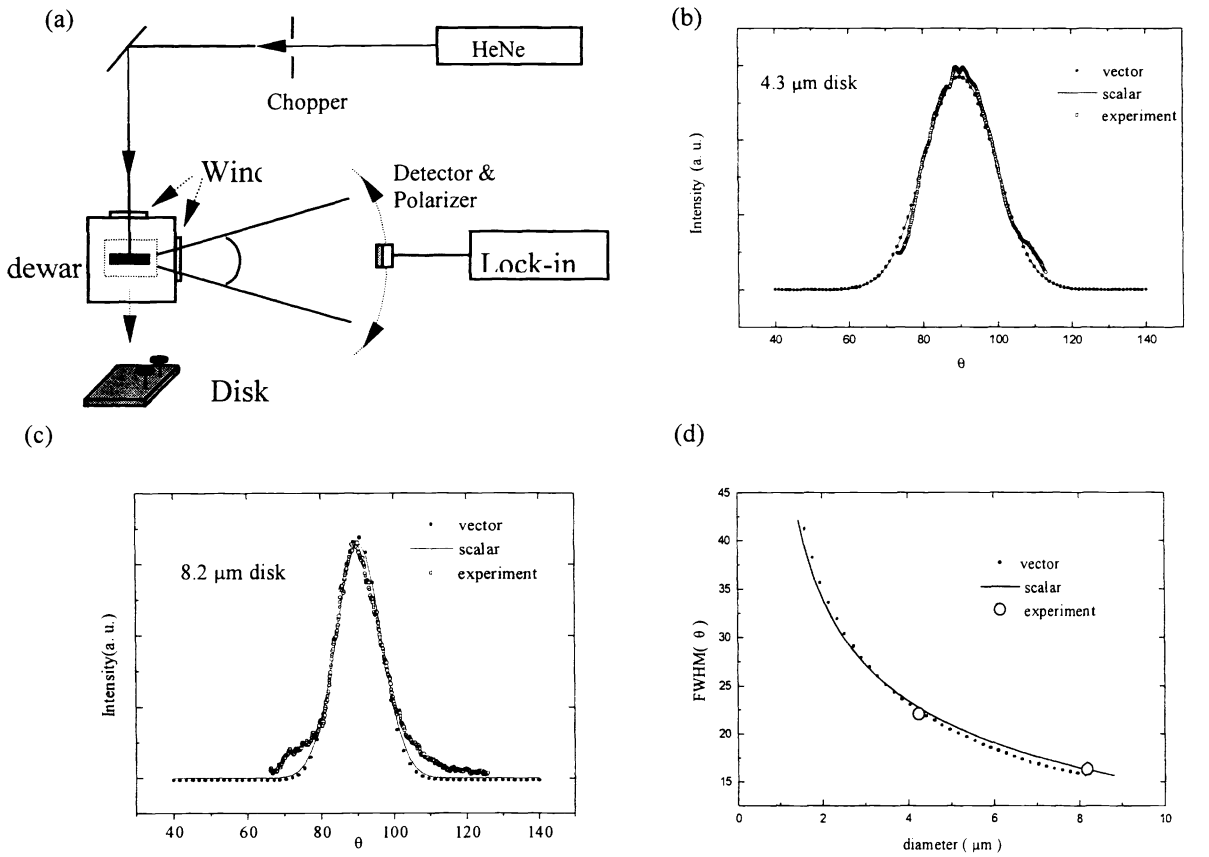

Figure 3: (a) Experimental setup for measuring the far-field pattern; (b) far-field pattern of a 4.3 μm micro-disk; (c) far-field pattern of a 8.2 μm micro-disk; (d) Comparison of theoretical predictions with the experimental data.

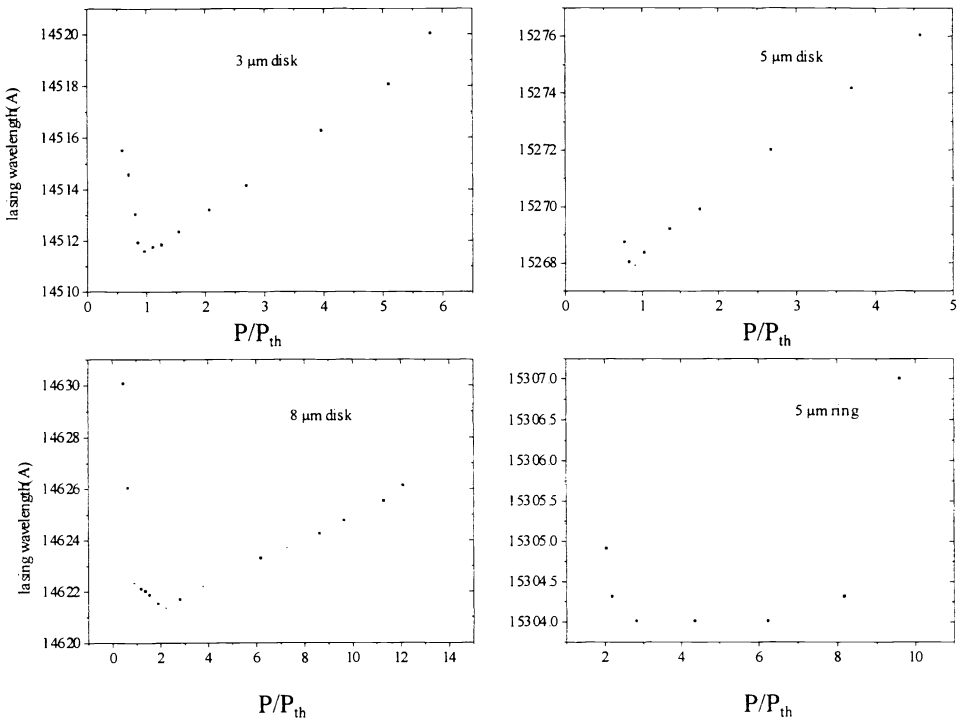

Figure 4: Lasing wavelengths of micro-disk and micro-ring lasers at different pump levels.

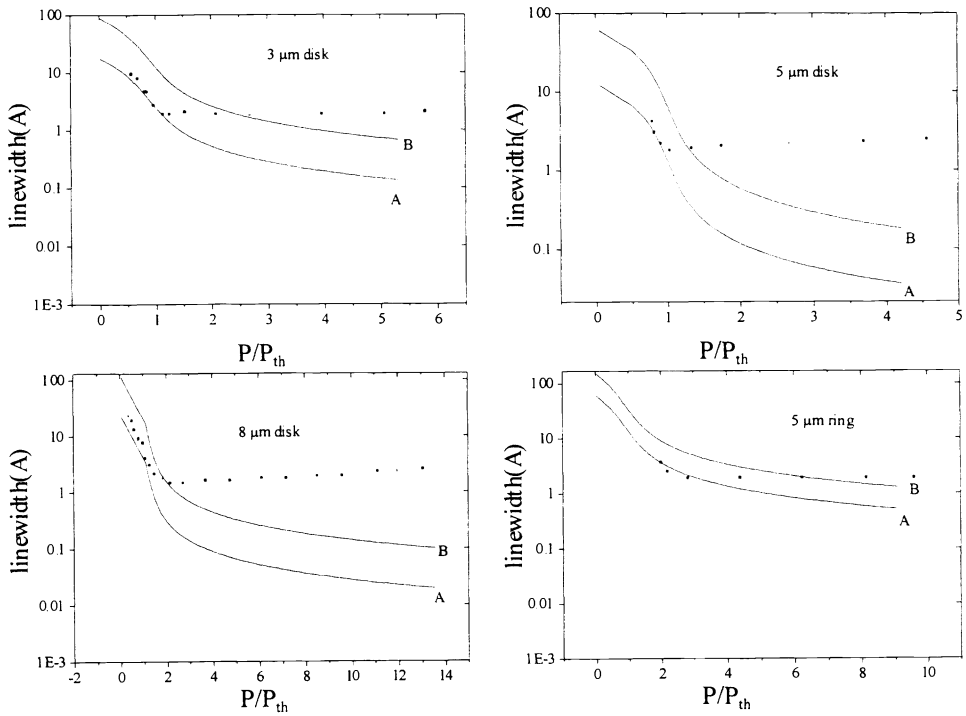

Figure 5: Lasing linewidths of micro-disk and micro-ring lasers at different pump levels. Dot points: experimental data; Solid line: theoretical predictions.

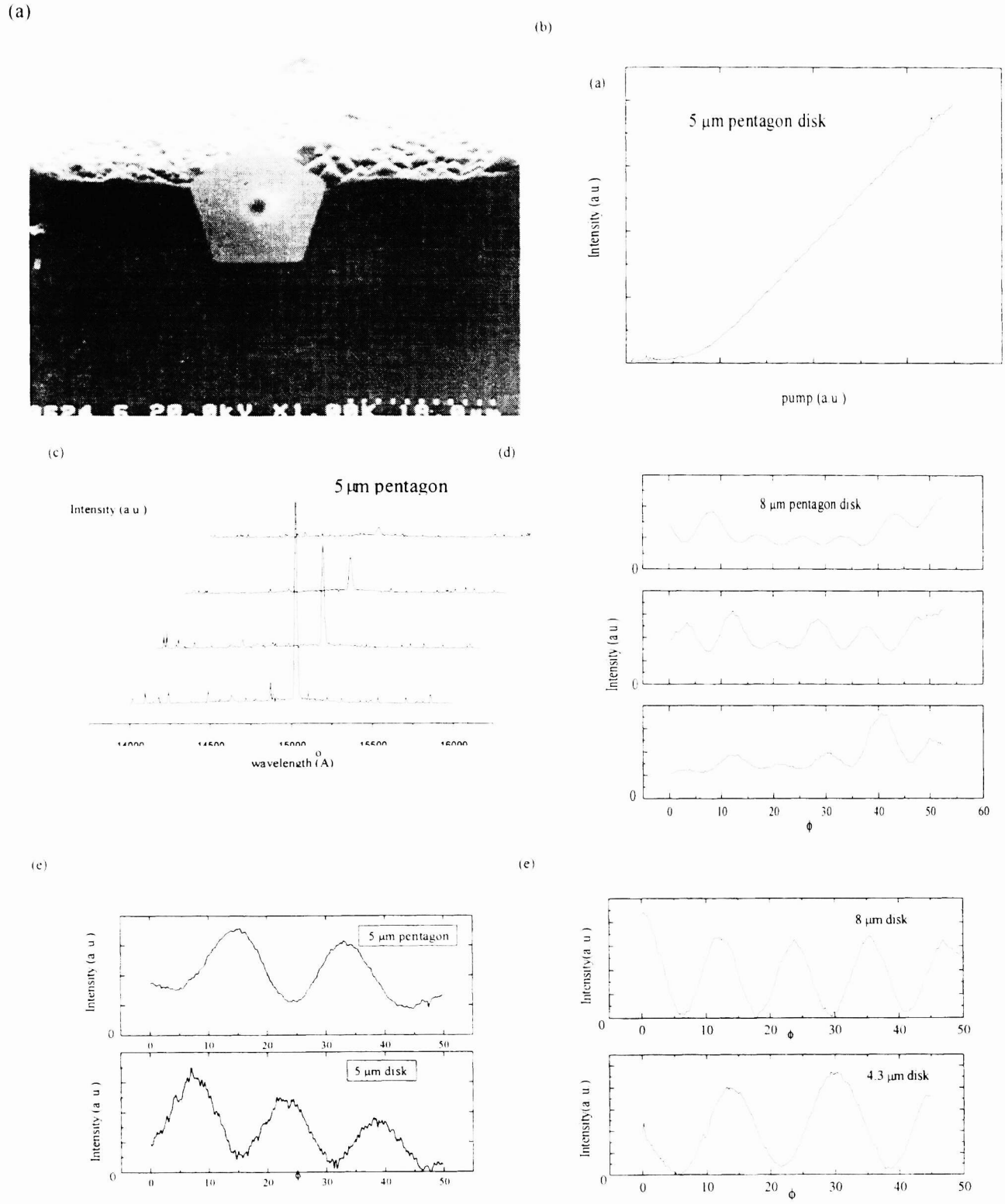

Figure 6: (a) SEM of a pentagon micro-laser on the wafer cleaved edge; (b) pump-output curve of a 5 μm pentagon micro-laser; (c) Lasing spectra of a 5 μm pentagon micro-laser; (d), (e), (f) far-field patterns along the ϕ direction for different micro-disk and micro- pentagon lasers.